Materials Physics and Mechanics 42 (2019) 646-655 Received: January 17, 2019

SHEAR ANISOTROPY IN Si-Cu INTERFACES ON THE ATOMIC SCALE

D. Johansson, P. Hansson, A. Ahadi, S. Melin*

Division of Mechanics, Lund Univeristy, PO Box 118, S22100 Lund, Sweden

*e-mail: solveig.melin@mek.lth.se

Abstract. Three dimensional molecular dynamics (MD) is used to model the mechanical response at the interface between a thin Cu coating resting on a base of Si. The copper coating is subjected to a displacement controlled shear load and the atom movements at the Si-Cu interface are monitored to investigate the effects of crystallographic anisotropy. The two crystals have the same crystallographic orientation, and two different interface normal directions are considered. The shear load is applied along different crystallographic directions to highlight the importance of crystallographic orientation for the mechanical response. The simulations are performed with the 3D MD free-ware LAMMPS. As the imposed displacement reaches a high enough magnitude, the Cu coating starts to slide over the Si base. Thus the atoms at the interface rearrange depending on loading direction and crystallographic orientation.

Keywords: Cu-coated Si, thin layers, 3D molecular dynamics, shear induced displacements, interface reorganazation, crystallographic anisotropy

1. Introduction

Over the past few decades there has arisen a need to design and, with high precision, manufacture nanoelectromechanical systems (NEMS). NEMS are used in a wide range of fields. One field is medicine where nanometer sized cantilevers have been employed to detect and neutralize specific cells, bacteria and viruses [1-3]. Other examples where NEMS are utilized are: in the manufacture of nanowires, in atomic force microscopy, in high density magnetic recording and in modern electronics such as solar cells, cell phones and computers [4-6]. Thus, in everyday life we are surrounded by components that have properties that are determined on the atomic level.

Experiments have shown that the material properties on the nanoscale are different from those on the macroscale. In a study of silver and lead nanowires it was observed that the elastic moduli of the nanowires started to increase when the diameters of the nanowires decreased below certain thresholds [7]. For nano-cantilevers made of chromium [8,9], and single crystalline Si [10] the opposite was observed, i.e. the elastic moduli decreased with the size of the cantilevers. In agreement with experimental studies, computer simulations have shown that the specimen size influences both the elastic modulus and the Poisson's ratio [11-13]. Moreover, it has been found that the size of the specimen also affects the stress and strain distributions in the vicinities of voids [14,15] and that also the strain rate affects the mechanical response [16,17]. Other factors that strongly affect the mechanical properties of nano-size components are lattice structure [18] and lattice orientations [16,19] of the material.

In a study of Cu coated Si films, subjected to shear displacement controlled loading by [20] it was observed that the character of the force-displacement curve (FDC) shifted as the lattice orientation of the Cu and/or the Si was changed. Also the mechanical properties of

http://dx.doi.org/10.18720/MPM.4252019_18
© 2019, Peter the Great St. Petersburg Polytechnic University
© 2019, Institute of Problems of Mechanical Engineering RAS

the coated film varied widely with lattice orientations and it was found that the differences in mechanical properties might be explained by how the Cu atoms at the Si-Cu interface relocate due to loading, i.e. are forced to move to adjacent, new positions. The aim of this paper is to further investigate how the relocations of the Cu atoms affect the mechanical properties of the coated film. In this paper only lattice orientation combinations where the Si crystal and the Cu crystal have the same crystallographic orientation, and where the interface normal is either pointing in the [010]-direction or the [-110]-direction, are considered.

2. Statement of the problem

MD simulations of base of cubic diamond Si coated with faced-centered cubic (FCC) Cu are performed, cf. Fig. 1. The dimensions of the film are about $217\text{Å}\times 217\text{Å}\times(\mathrm{h_{Si}}+\mathrm{h_{Cu}})$, where $\mathrm{h_{Si}}$ and $\mathrm{h_{Cu}}$ are the heights of the Si base and Cu coating with $\mathrm{h_{Si}}\approx 28.5\text{Å}$ and $\mathrm{h_{Cu}}\approx 42.5\text{Å}$, respectively. The two latter measures are chosen large enough to ensure that the top and the bottom atomic layers, where constraints are imposed, do not directly influence the Si-Cu interface. The measure 217Å is roughly the length of 60 and 40 unit cells in the $\langle 100\rangle$-directions for Cu and Si, respectively with the lattice parameter $a_{\mathrm{Cu}}\approx 3.62\text{Å}$ for Cu and for Si $a_{\mathrm{Si}}\approx 5.43\text{Å}$.

The simulations are performed using the molecular dynamics freeware LAMMPS [21,22] and the inter-particle potentials are taken from Jelinek et al. [23]. All simulations start with a relaxation of the atomic structure for 10000 time steps, with one time step equal to 1fs, thus giving a relaxation time equal to 10ps. This relaxation time is considered enough as judged from monitoring the movements of individual atoms. When the relaxation is completed all atoms in the two bottom Si atom layers are fixed in all directions, cf. Fig. 1, and this constraint is kept through the simulations. The top two Cu atom layers are given a constant velocity v_z in the *z*-direction, with $v_z = 0.02172\text{Å/ps}$.This causes a displacement controlled shear loading, with a constant strain rate of $\dot{\varepsilon} = 10^8\text{s}^{-1}$. All other atoms are unconstrained. The simulations employ a NVT integrator, i.e. keeping the number of atoms *N*, the volume *V* and the temperature *T* constants. A Nose-Hoover thermostat [24] holds the temperature *T* constant at 300K.

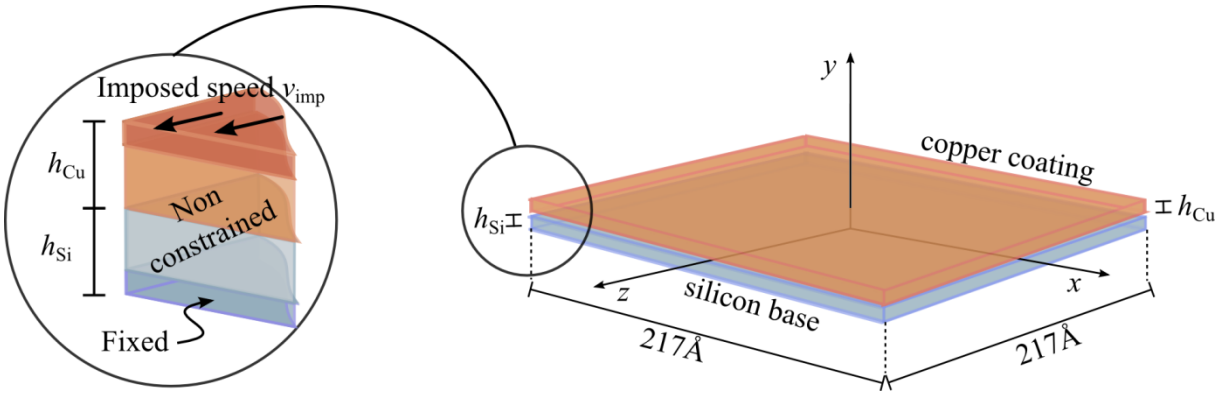

Fig. 1. Schematic illustration of the simulated films. The atoms within the dark copper colored volume and the atoms within the dark blue colored volume according to the zoom-in to the left hold the boundary constraints. Figure adopted from [20]

The load cases that are studied in this paper are listed in Table 1, where for each simulation the crystal orientations for Cu and Si are equal. The simulations are named with a letter followed by a number, with the letter determining the interface normal. If the simulation

name begins with the letter A the interface normal is in the [010]-direction, and if the simulation name begins with the letter B the interface normal is in the [110]-direction. The number in the simulation name tells the approximate angle, β, between the direction of the applied load, i.e. the *z*-direction, and the [101]-direction that is closest to the *z*-direction in the Cu coating. The time step is kept at 1fs and after the initial relaxation phase the simulations continues for 500000 time steps, equal to 500ps. The number of atoms in the simulations is 174489 Cu-atoms and 70515 Si-atoms.

Table 1. Considered load cases with corresponding crystallographic orientations along the *x*, *y* and *z* directions

Sim.	Cu lattice directions			Si lattice directions		
	x-dir	*y*-dir	*z*-dir	*x*-dir	*y*-dir	*z*-dir
A0	[10-1]	[010]	[101]	[101]	[010]	[101]
A34	[50-1]	[010]	[105]	[501]	[010]	[105]
A45	[100]	[010]	[001]	[100]	[010]	[001]
B0	[00-1]	[-110]	[110]	[00-1]	[-110]	[110]
B35	[11-2]	[-110]	[111]	[11-2]	[-110]	[111]
B90	[110]	[-110]	[001]	[110]	[-110]	[001]

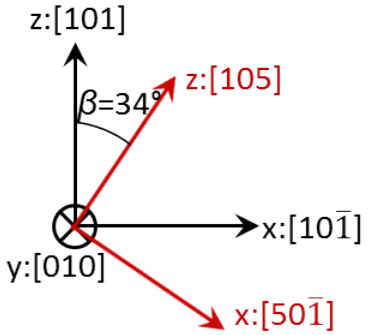

Fig. 2. Lattice directions in simulations A0 (black) and A34 (red)

This is illustrated for two different simulations A0 and A34 in Fig. 2. The difference between the load cases is merely a rotation of the loading direction with respect to the crystal orientation around the *y*-axis, i.e. the normal to the surface, an angle $\beta = 34^\circ$.

3. Numerics

Inter-atomic potential. The atomic interactions are simulated by a Modified Embedded Atom Method (MEAM) potential [25] which is an extension of the Embedded Atom Method [26,27]. In this study the potential parameters are taken from Jelinek et al. [23] using the AlSiMgCuFe.meam and library.meam files, as implemented in LAMMPS. When employing a MEAM potential, the total energy E of the ensemble is approximated by the sum of all individual atomic energies E_i, cf. Eq. 1. The energy of atom i consists of two parts; one embedding part and one pair potential part, cf. Eq. 2.

$$E = \sum_i E_i \,. \tag{1}$$

$$E_i = F_i(\bar{\rho}_i) + \frac{1}{2}\sum_{j \neq i} \Phi(r_{ij}) \,. \tag{2}$$

In Eq. 2 the embedding part F_i represents the energy that an ion of atom i's type gets when the ion is embedded by the electrons in the vicinity of its position. Furthermore, $\overline{\rho}_i$ denotes the background electron density at the position of atom i, Φ_{ij} represents the pair potential and r_{ij} the interatomic distance between atom i and atom j.

Force Calculations. The force acting om atom i in the *z*-direction, f_z, needed to obtain a prescribed displacement in the *z*-direction, δ_{ij}, is calculated as:

$$f_z = \sum_{i \in \mathrm{ALL}} f_{z_i} - \sum_{i \in \mathrm{TOP}} f_{z_i}, \tag{3}$$

where ALL and TOP are two groups of atoms consisting of all atoms in the simulation and the atoms in the top two Cu layers, respectively. To smoothen out the FDCs, f_z is filtrated by applying a Savitzky-Golay filter [28]. The convolution in a Savitzky-Golay filter is that the data is divided into subsets of adjacent data-points from which a low degree polynomial is fitted by applying the least square method. To achieve distinct FDCs without losing the nature of the curves and smoothen out the extremes, the polynomial degrees and the interval lengths of the adjacent data-points sets are determined after optical evaluations.

4. Results and discussion

To investigate the mechanical behavior of the Si-Cu interface, the FDC curves are calculated for the different lattice orientations given in Table 1. From these the behavior of the thin film systems can be described and the mechanical properties derived. Also the exact atomic motions of a number of Cu atoms in the atomic layer closest to the Si substrate at the interface have been studied in order to explain the observations made.

Force displacement curves (FDC). As the Cu-Si is loaded, the Cu coating at some point starts to slide on top of the Si base. Fig. 3 shows the FDCs for all cases listed in Table 1 with the force on the vertical axis according to Eq. 3 versus imposed displacement δ_{imp} in the *z*-direction on the TOP atoms. As seen the curves are oscillating. The oscillations arise due to the fact that both the Si base and the Cu coating are crystalline and, as the Cu coating moves over the Si base, the conformity in atomic positions at the interface between Cu and Si vary, resulting in large variations in the applied force on the Cu coating necessary to obtain shearing.

When comparing the FDCs for group A in Fig. 3a) it can be seen that all three curves have similar shape, with an initial almost linear part followed by a oscillating part with high amplitude, i.e. large variations in applied force. The curves show an increase in maximum force but a decrease in amplitude with increasing β. The frequency of the oscillations, however, do not differ much in-between the three cases. The reasons for the different appearances of the curves will be further discussed in Paragraph 4.

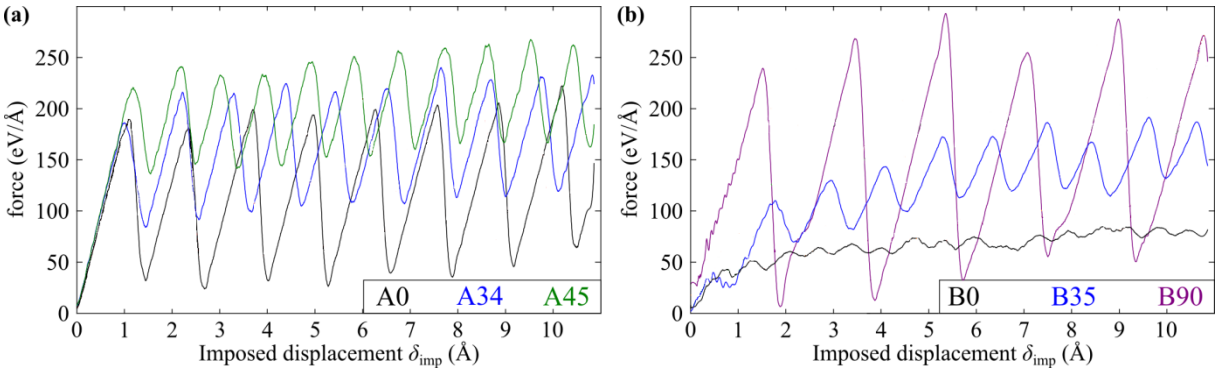

Fig. 3. Force-displacement curves for a) group A and b) group B

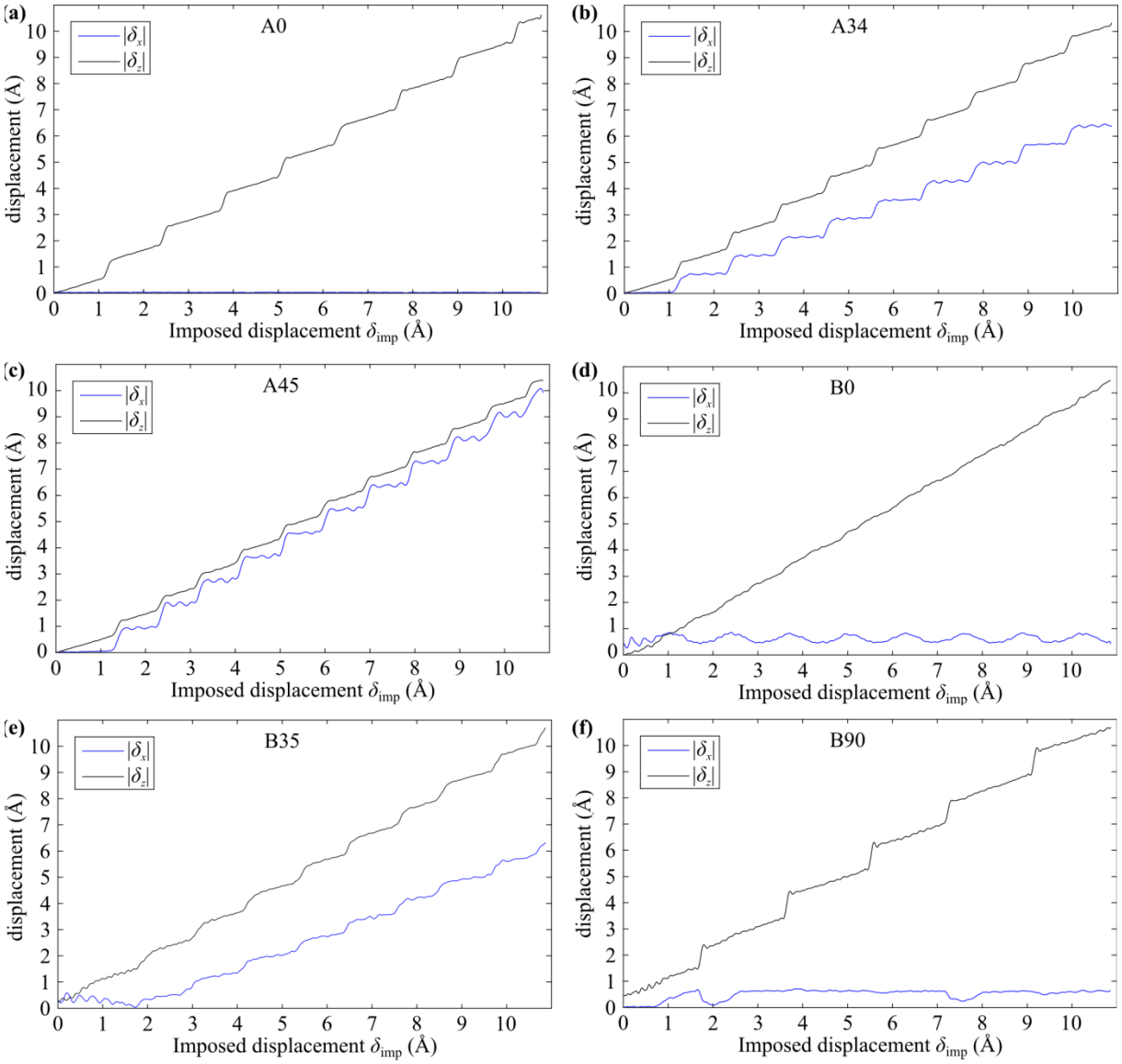

Fig. 4. Displacements of the monitored Cu atoms in the Cu layer closest to the Si atoms in the *x*- and *z*-directions versus imposed displacement

For group B, seen in Fig. 3b), much larger variations in-between the three different curves can be observed, as compared to group A. Simulation B9 shows a behavior similar to that of group A, with high magnitude of force and oscillations with large amplitudes. Simulation B0, however, shows very low forces and very low amplitude of the oscillations, resulting in an almost smooth FDC curve. Simulation B35 has a very low first peak of the FDC, but after this initial weak behavior it shows a behavior somewhere in between simulations B90 and B0, with moderate amplitudes of the oscillations. The frequency of the oscillations decreases markedly with increasing β. The different curve appearances are further discussed in Paragraph 4.

Displacements in the Cu-Si interface. To better understand the different shapes of the FDC curves, the average displacements in the interface of the 21 Cu atoms closest to the coordinate system Origin in the Cu layer closest to the Si-atoms prior to loading were monitored throughout the simulations. In Fig. 4 the average *x*- and *z*-displacements, cf. Fig. 1, are plotted vs. the imposed displacement, δ_{imp}.

In Figure 4a) the deformation behavior at the Si-Cu interface can be seen for simulation A0. In this case the Cu atoms slide in the *z*-direction only, with δ_x approximately zero. The displacement occurs in a step wise manner, were δ_z first slowly increases before a sudden rapid increase in δ_z occurs. These sudden steps in δ_z correspond to the large drops in force seen in Fig. 4a). Similar behavior is also observed in the A34 and A45 simulations for the *z*-direction. However, in the *x*-direction different behavior can be observed for the different cases. In the A45 simulation the δ_x curve almost follows the δ_z curve, meaning that an approximately equal amount of glide in the *x*- and z-directions occurs. Thus, in this case, the global displacement appears in an angle of approximately 45° to the loading direction. Similar results are also observed for the A34 direction but with a smaller amount of deformation in the *x*-direction than for the A45 simulation. The explanation for this behavior is described in paragraph 4 and in Fig. 5.

For group B the results of the deformation at the interface are seen in Fig. 4d-f). Also here, as seen in Fig. 4b), large differences between the simulations are at hand. In the B0 simulation the δ_z curve is very smooth, without any irregularities which corresponds to what was observed in the FDC curve. For the B35 and B90 simulations, however, the same irregularities that were observed in group A was found which, again, are in correspondence to the observations in the FDC curves. Here simulations B0 and B90 show similar behavior with only small variations in the δ_x value, indicating that the glide almost entirely occurs in the loading direction. However, for the B35 simulation also the δ_z value increased in an irregular pattern, similar to what was found in the A34 simulation, showing that in this case the total deformation occurred at some angle to the loading direction. The explanations for these behaviors are described in Paragraph 4 and in Fig. 6.

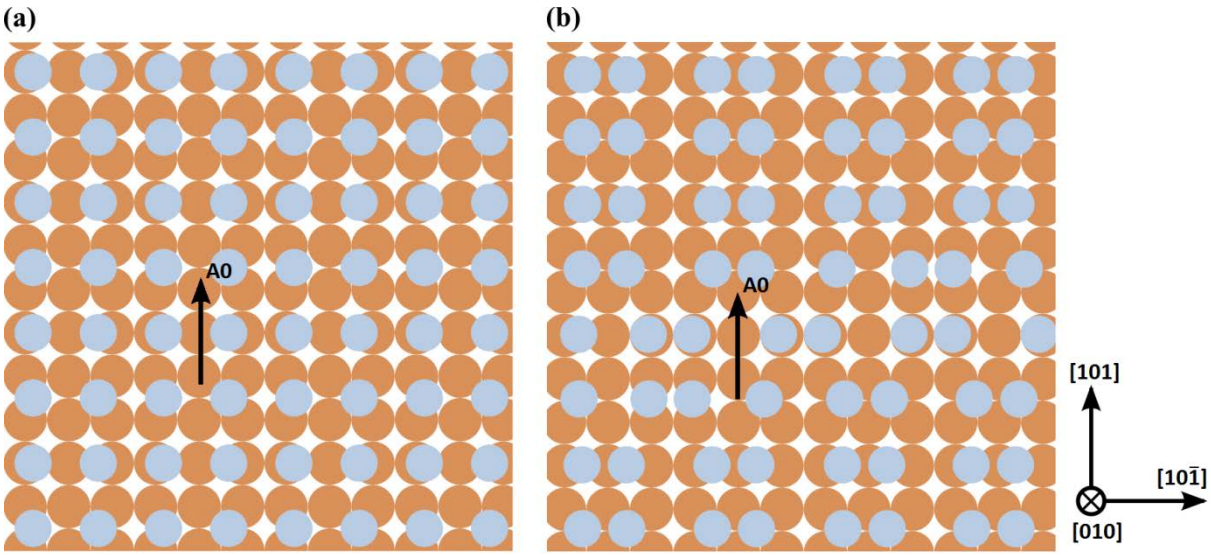

Fig. 5. Atomic positions in the Si-Cu interface for simulation A0. a) after relaxation and b) at $\delta_{imp} \approx 0.5\text{Å}$. Note that the *y*-direction is [010]

Atomic movements in the interface. In Figure 5 the atomic movements in simulations A0 can be seen, with the arrows indicating the loading direction, i.e. the *z*-direction. The copper colored circles correspond to the Cu atom positions and the blue corresponds to the Si atom positions. Note that only the positions of the atoms and not their relative size are

depicted. Fig. 5a) corresponds to the atomic positions at the interface directly after relaxation and Fig. 5b) to the atomic positions at $\delta_{imp} \approx 0.5\text{Å}$. It can clearly be seen that the Si atoms during deformation rearrange so that most of them ends up at positions in between the copper atoms, and only atomic movements in the *z*-direction occurs, cf. Fig. 4a).

It can also be concluded that, for this deformation to be able to take place, the Cu atoms must move over the Si atoms, with most of the Cu atoms passing in-between two Si atoms. This gives rise to oscillating displacements in the *y*-direction. It is this mechanism that gives rise to the oscillations in the curves in Fig. 3.

In Figure 6 the atomic arrangements in simulations a) B35 and b) B0 and B90, can be seen at $\delta_{up} \approx 34^\circ$, with the arrows indicating the loading directions, i.e. the *z*-direction in each simulation. For simulation B35 it can clearly be seen that the Si and Cu atoms arrange in parallel lines, at an angle β approximately 35° to the loading direction. In this direction the obstacle of deformation are less that for group A, resulting in a smoother deformations especially in δ_x component. This explains the behavior observed in Fig. 4e) where deformation occurs both in the *x*- and *z*-directions, and the amount of deformation in the *x*-direction gives a total deformation at an angle 35 to the loading direction *z*, agrees with the angle found in Fig. 6. Also the appearance of the FDC curve can be explained, with the smaller oscillations and lower forces needed as compared to simulation group A, due to this direction of easier deformation.

For simulation B0, cf. Fig. 6b), it can be observed that also here the Si and Cu atoms are positioned in channels parallel with each other, but in this case perpendicular to the loading direction. This results in that the atoms act as walls, hard to climb over, resulting in high forces and large amplitudes of the oscillations cf. Fig. 3b). This deformation mechanism also explains the behavior observed in Fig. 4d) with almost no deformation in the *x*-direction and large steps in the deformation in the *z*-directions due to the difficulties for the atoms to pass theses walls. Fig. 6b) also includes the B90 simulation. In this case the loading direction is parallel to the channels of the Si and Cu atoms. As a result low forces are needed to deform the interface, resulting in oscillations with small amplitude as seen in Fig. 3b). This also results in little deformation in the *x*-direction as seen in Fig. 4f).

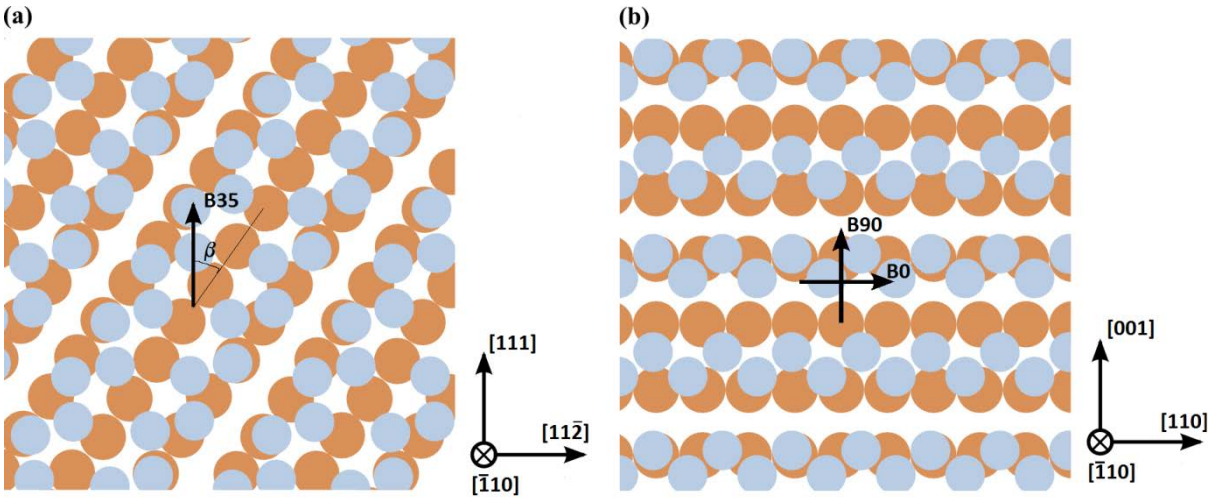

Fig. 6. Atomic arrangements in the Si-Cu interface for simulations a) B35and b) B0 and B90. Note that the *y*-direction is [-110]

Mechanical properties. In Table 2 some mechanical properties extracted from the simulations are listed. The properties include the applied displacement at the first peak; and

the force at the first peak, f_{1p}, taken from in the FDCs shown in Fig. 3. Also the initial stiffness K_{init} i.e. the initial slope of the curve, and the initial shear resistance G_{init} were calculated in accordance with [20] are given in Table 2.

Table 2. Mechanical properties. See [20] for definitions

Sim.	A0	A34	A45	B0	B45	B90
Displacement to first peak δ_{1p} (Å)	1.1	1.1	1.2	0.7	0.5	1.5
Force at first peak f_{1p} (eV/Å)	190	187	220	43	40	240
Initial stiffness K_{init} (N/m)	2870	2880	3070	1090	1210	2310
Initial shear resistance $\overline{G}_{init}$ (Gpa)	26.9	236.5	28.3	10.5	11.1	21.1

For simulation group A it is seen that δ_{1p} is roughly the same for all three simulations. However, f_{1p} are not similar, with simulation A45 having the highest value and A0 the lowest. This means that the lowest shear force is needed to initiate and maintain glide in the interface is for the A0 case and the highest for the A45 case. The same trend can be seen regarding stiffness and shear resistance, with A45 having the highest values and A0 the lowest. The results are consistent with what was discussed in Paragraph 4 and with the observations from Fig. 5.

Looking at the values in Table 2 for group B a much larger variation between the three simulations is seen. The lowest δ_{1p} and f_{1p} are obtained for the B35 case and the highest for the B90 case, with the B90 values being superior far higher to the values from the B0 and B35 simulations. Regarding the initial stiffness and shear resistance the B90 values are more than the double magnitude as compared to B0 and B35. Also these results are consistent with what was discussed in Paragraph 4, where the results can be explained from the atomic configurations in Fig. 6, describing the movements of the atoms at the interface.

6. Summary

In this paper the movements of the Cu atoms at the interface of a Cu coated Si base, subjected to a displacement controlled shear loading, have been studied. It was found that, as the load reached a high enough magnitude, the Cu coating started to slide over the Si base. Two different lattice orientation combinations, loaded in three different lattice directions for each orientation were investigated.

The results show that the anisotropy is high and that the mechanical properties vary widely between different lattice orientation combinations and loading directions. As the Cu coating slides over the Si base, the shear force necessary to make the Cu coating slide oscillates, were the oscillations arise because both the Si base and the Cu coating are crystalline, meaning that, at the atomic level, the surfaces have a periodic structure. Both the amplitude and the frequency of the oscillations vary highly between the different cases and the different behaviours could be related to the discrete atomic structure at the interface.

Also the average in-plane displacements of a group of Cu atoms in the atomic plane closest to the Si base were monitored. It was found that, for certain combinations of loading direction and crystallographic orientation, the displacements of the Cu atoms occurred in the loading direction, only. However, for other combinations of loading direction and crystallographic orientation, the resulting displacement occurred at an angle to the loading direction, with the extreme case of resulting displacement direction at an angle 45º to the loading direction. The displacements were monitored for each case and the displacement curves were found to correlate with the corresponding force-displacement curves; sudden

steps in the displacement curves could be correlated to the oscillations in the force-displacement curves. The observation was that smooth force-displacement curves correlate to smooth displacement curves, and that the sudden jumps in displacement curves correlate to sudden drops in force in the force-displacement curves.

Acknowledgements. *No external funding was received for this study.*

References

[1] Ilic B, Czaplewski D, Craighead HG, Neuzil P, Campagnolo C, Batt C. Auto-parametric optical drive for micromechanical oscillators. *Appl. Phys. Lett*. 2000;77(3): 450-452.
[2] Reich D, Tanase M, Hultgren A, Bauer L, Chen C, Meyer G. Cell manipulation using magnetic nanowires. *J. Appl. Phys.* 2003;93(10): 7275-7280.
[3] Gupta A, Akin D, Bashir R. Single virus particle mass detection using microresonators with nanoscale thickness. *Appl. Phys. Lett*. 2004;84(11): 1976-1978.
[4] Sellmyer D, Zheng M, Skomski R. Effects of surface morphology on magnetic properties of Ni nanowire arrays in self-ordered porous alumina, *J. Phys.: Condensed Matter*. 2001;13(25): R433.
[5] Stowe T, Yasumura K, Kenny T, Botkin D, Wago K, Rugar D. Attonewton force detection using ultrathin silicon cantilevers. *Appl. Phys. Lett*. 1997;71(2): 288-290.
[6] Chau R, Doyle B, Datta S, Kavalieros J, Zhang K. Integrated nanoelectronics for the future. *Nature materials.* 2007;6: 810-812.
[7] Cuenot S, Fretigny C, Demoustier-Champagne S, Nysten B. Surface tension effect on the mechanical properties of nanomaterials measured by atomic force microscopy. *Phys. Rev. B.* 2004;69(16): 165410.
[8] Nilsson SG, Sarwe EL, Montelius L. Fabrication and mechanical characterization of ultrashort nanocantilevers. *Appl. Phys. Lett*. 2004;83(5): 990-992.
[9] Nilsson SG, Borris X, Montelius L. Size effects on Young's modulus of thin chromium cantilevers. *Appl. Phys. Lett.* 2004;85(16): 3555-3557.
[10] Li X, Ono T, Wang Y, Esashi M. Ultrathin single-crystalline-silicon cantilever resonators: fabrication technology and significant specimen size effects on Young's modulus. *Appl. Phys. Lett*. 2003;83(15): 3081-3083.
[11] Liang H, Upmanyu M, Huang H. Size-dependent elasticity of nanowires: non-linear effects. *Phys. Rev. B.* 2005;71(24): 241403.
[12] Olsson PAT, Melin S, Persson C. Atomistic simulations of tensile and bending properties of single-crystal BCC-Iron nanobeams. *Phys. Rev. B*. 2007;76(22): 1-15.
[13] Ahadi A, Melin S. Size dependence of the Poisson's ration in single-crystal fcc copper nanobeams. *Comput. Mater. Sci*. 2016;11: 322-327.
[14] Johansson D, Hansson P, Melin S. Stress analysis around a through crack shaped void in a single crystal copper strip coated on an infinitely stiff material using molecular dynamics. *Engin. Fract. Mech.* 2014;116: 58-68.
[15] Johansson D, Hansson P, Melin S. Stress and displacement configurations in the vicinity of a void in a nanometer copper strip. *Engn. Fract. Mech*. 2015;152: 139-146.
[16] Kim W, Cho M. Surface effect on the self-equilibrium state and size-dependent elasticity of FCC thin films. *Modelling and Sim. Mater. Sci. and Engn.* 2010;18(8): 085006.
[17] Park HS, Zimmerman JA. Modeling inelasticity and failure in gold nanowires. *Phys. Rev. B*. 2005;72(5): 054106.
[18] Callister WD, Rethwisch DG. *Fundamentals of materials science and* engineering. John Wiley & Sons; 2012.

[19] Liang H, Liu G, Han X. Atomistic simulation on the stiffening and softening mechanism of nanowires. In: Liu G, Tan V, Han X. (eds.) *Computational Methods*. Dordrecht: Springer; 2006. p.1667-1672.
[20] Johansson D, Hansson P, Melin S. Lattice optimization of Si-Cu interfaces on atomic scale. *Comp. Mater. Sci.* 2017;128: 59-66.
[21] Plimpton S. Fast parallel algorithms for short-range molecular dynamics. *J. Comp. Phys.* 1995;117(1): 1-19.
[22] Plimpton S, Thompson A, Crozier P, Kohlmeyer A. *LAMMPS Molecular Dynamics Simulator*. Available from: http://lammps.sandia.gov/ [Accessed 29th November 2019].
[23] Jelinek B, Groh S, Horstemeyer MF, Houze J, Kim SG, Wagner GJ, Moitra A, Baskes MI. Modified embedded atom method potential for Al, Si, Mg, Cu, and Fe alloys. *Phys. Rev. B*. 2012;85(24): 245102.
[24]Tadmor EB, Miller RE. *Modeling materials: continuum, atomistic and multiscale techniques.* Cambridge University Press; 2011.
[25] Baskes MI. Modified embedded-atom potentials for cubic materials and impurities. *Phys. Rev. B.* 1992;46(5): 2727.
[26] Daw MS, Baskes MI. Semiempirical, quantum mechanical calculation of hydrogen embrittlement in metals. *Phys. Rev. B.* 1983;50(17): 1285.
[27] Daw MS, Baskes MI. Embedded-atom method: Derivation and application to impurities, surfaces, and other defects in metals. *Phys. Rev. B.* 1984;29(12): 6443.
[28] Savitzky A, Golay MJ. Smoothing and Differentiation of Data by Simplified Least-Squares Procedures. *Analytical Chem.* 1964;36(8): 1627-1639.
[29] Stukowski A. Visualization and analysis of atomistic simulation data with OVITO- the Open Visualization Tool. *Modelling and Simul. Mater. Sci. Eng*. 2010;18(1): 015012.